ORIGINAL ARTICLE

Radical crossover reactions of alkoxyamine-based dynamic covalent polymer brushes on nanoparticles and the effect on their dispersibility

Tomoya Sato[1,2], Tomoyuki Ohishi[1], Yuji Higaki[3], Atsushi Takahara[2,3] and Hideyuki Otsuka[1,2]

The dynamic covalent exchange reactions of side chains in polymer brushes on nanoparticles were successfully demonstrated, and the dispersibility of the nanoparticles after the exchange reactions was investigated in some solvents. A polymer brush with exchangeable alkoxyamine side chains was prepared by surface-initiated atom transfer radical polymerization on silica nanoparticles. Fluorinated and ionic polymers were grafted to the polymer brush via radical exchange reactions of alkoxyamine moieties. The chemical composition of the polymer brushes on nanoparticles before and after the exchange reactions was investigated by X-ray photoelectron spectroscopy (XPS). The XPS measurements indicated that the side chains of the polymer brushes were converted to the corresponding polymers. In addition, the grafted side chains could be detached from the surface of the nanoparticles through a further radical exchange process by treating with alkoxyamines. The XPS results indicate that the structure of the de-grafted polymer brush is nearly the same as the original, thus demonstrating the reversibility of the reactions. Furthermore, the dispersibility of the nanoparticles in solution could be changed by the reversible grafting reactions.

INTRODUCTION

Nanoparticles, nanotubes and nanosheets have recently become the subject of increasing research because of their applications to electronics, photonics, the reinforcement of polymeric materials and biomedical fields.[1–4] For these applications, the dispersibility of the nanomaterials in specific media is important. Accordingly, intense research into the introduction of functional groups on the surface of nanomaterials to modify their dispersion properties has been performed. One practical approach is surface modification with polymer brushes.[5,6] The structure of a polymer brush contains polymer chains directly attached to organic or inorganic materials. Therefore, modified polymer chains can cover the surface of the nanomaterials and prevent their aggregation due to the steric hindrance of perpendicularly stretched polymer chains. Furthermore, polymer brushes with a high graft density[7–12] have been synthesized using the grafting from method with precise polymerization techniques.[13–16] To date, various polymer brushes have been prepared on the surface of nanomaterials.[17–22] In addition, polymer brushes with convertible structures[23] have been developed to allow the modification of their properties.[24–35] For example, the surface structure and properties of ionic polymers can be altered by changing the solution pH.[24–26] Nanomaterials with ionic polymer brushes can be switched between a dispersed and an aggregated state in an aqueous solution. Another strategy is to change the temperature to control the

nanomaterials by exploiting the phase transition of the polymer; when nanoparticles with poly(N-isopropylacrylamide) brushes are heated and cooled, they show changes in their dispersibility and structure.[32–35] However, most of the previously reported systems cannot reversibly alter the structures and compositions of the brushes, limiting their applications.

Recently, the use of reversible bonding for molecular design and synthesis has been studied[36] to fabricate materials with new characteristics. In particular, chemistry based on reversible covalent bonds, known as 'dynamic covalent chemistry', has attracted much attention because it allows the creation of novel molecules and materials that could not be produced by traditional methods.[37–39] Most dynamic covalent bonds are stable under ambient conditions, while they begin to equilibrate between states when external stimuli, such as heating, chemical additions or light irradiation, are applied. Therefore, materials containing dynamic covalent bonds are stable, but they can react further. In particular, when the concept of dynamic covalent chemistry is applied to polymeric materials,[40,41] polymers that have reorganizable structures, compositions and properties are designed.

One typical example of a dynamic covalent system is the reversible C–ON bond formation of alkoxyamine units derived from stable nitroxide radicals.[42–45] Alkoxyamine derivatives can form carbon and nitroxide radicals on heating due to the homolytic cleavage of the covalent C–ON bond. These are well-known and commonly used as

[1]Department of Organic and Polymeric Materials, Tokyo Institute of Technology, Tokyo, Japan; [2]Department of Chemistry and Biochemistry, Graduate School of Engineering, Kyushu University, Fukuoka, Japan and [3]Institute for Materials Chemistry and Engineering, Kyushu University, Fukuoka, Japan
Correspondence: Professor A Takahara, Institute for Materials Chemistry and Engineering, Kyushu University, 744 Motooka, Nishi-ku 819-0395, Japan or Professor H Otsuka, Department of Organic and Polymeric Materials, Tokyo Institute of Technology, 2-12-1 Ookayama, Meguro-ku, Tokyo 152-8550, Japan.
E-mail: takahara@cstf.kyushu-u.ac.jp or otsuka@polymer.titech.ac.jp
Received 11 July 2015; revised 17 August 2015; accepted 18 August 2015; published online 14 October 2015
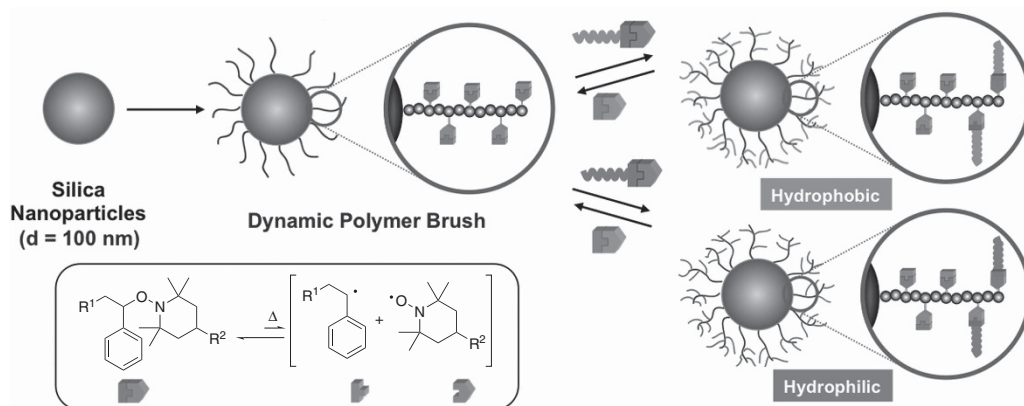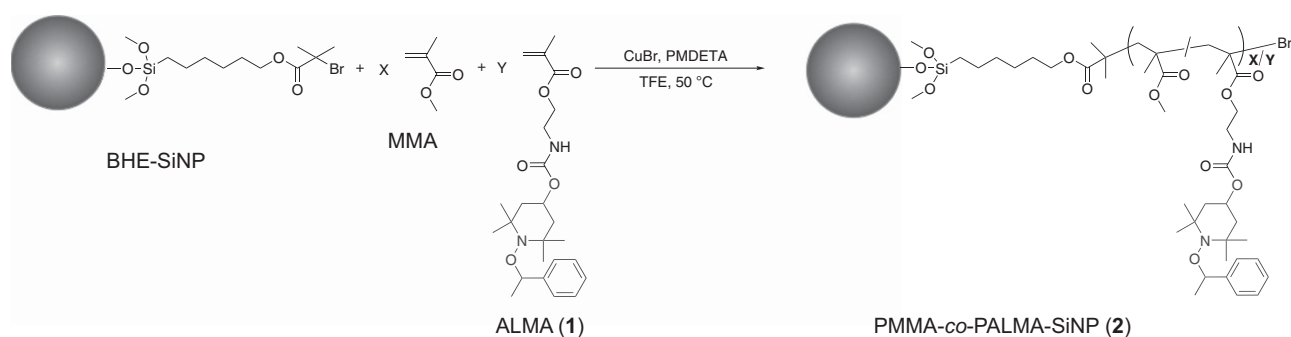
Figure 1 Alkoxyamine-based dynamic covalent exchange reactions on nanoparticles. A full color version of this figure is available at *Polymer Journal* online.

Scheme 1 Preparation of an alkoxyamine-based dynamic covalent polymer brush on silica nanoparticles. ALMA (**1**), 2,2,6,6-tetramethylpiperidine; BHE, 2-bromo-2-methyl)propionyloxyhexyltriethoxysilane; MMA, methyl methacrylate; PMMA, poly(methyl methacrylate); SiNP, silica nanoparticle; TFE, trifluoroethanol. A full color version of this scheme is available at *Polymer Journal* online.

unimolecular initiators or chain end structures in nitroxide-mediated radical polymerization (NMRP).[14,42] Recently, alkoxyamine-based reorganizable structures, such as linear,[46–48] cyclic,[49] grafted,[50,51] cross-linked[52–57] and star-shaped[58,59] polymers, have been developed. In these systems, alkoxyamine-based dynamic covalent polymers satisfy the conditions of stability under ambient conditions and radical reactivity. In addition, several dynamic covalent reactions on the surface and at the interface of materials have been reported more recently.[60–68] These reactions are applicable to surface property changes of nanomaterials.[69–72]

In this study, we report the reversible control of the chemical composition of the surface of silica nanoparticles (SiNPs) and the effect of the dynamic covalent polymer brushes on the dispersibility of the nanoparticles in solution. The system investigated in this study is based on the dynamic covalent exchange reactions. A schematic representation of the reversible polymer grafting system through dynamic covalent exchange reactions of alkoxyamine units is shown in Figure 1.

EXPERIMENTAL PROCEDURE
Materials
Alkoxyamine derivatives, 4-(methacryloyloxyethylcarbamyl)-1-((1′-phenylethyl)oxy)-2,2,6,6-tetramethylpiperidine (ALMA, **1**)[58] and 4-methoxy-1-((1′-phenylethyl)oxy)-2,2,6,6-tetramethylpiperidine (**5**),[50] were prepared as previously reported. The surface initiator, (2-bromo-2-methyl)propionyloxyhexyltriethoxysilane (BHE), and the suspension of initiator-modified SiNPs were prepared according to reported procedures.[12,21,22] Methyl methacrylate (MMA, 98+%) and anisole (99+%) were purchased from Wako Pure Chemical Industries (Osaka, Japan) and were purified by distillation under reduced pressure over calcium hydride. 2,3,4,5,6-Pentafluorostyrene (99%) was purchased from

Sigma-Aldrich Japan (Tokyo, Japan) and was purified by distillation under reduced pressure over calcium hydride. 4-Vinylpyridine (95+%) was purchased from Tokyo Chemical Industry (Tokyo, Japan) and was purified by distillation under reduced pressure over calcium hydride. Free initiator, ethyl 2-bromoisobutyrate (98+%) was received from Tokyo Chemical Industry (Osaka, Japan) and was distilled under reduced pressure. Cu(I)Br (99+%) was purchased from Wako Pure Chemical Industries and was purified by repeated stirring in acetic acid (Wako Pure Chemical Industries 99+%), washed with ethanol (Wako Pure Chemical Industries 99+%) and then dried *in vacuo*. The SiNP suspension (100 nm diameter) was kindly supplied by Nissan Chemical Industries (Chiba, Japan). All other reagents were purchased from commercial sources and were used as received.

Measurements
[1]H (400 MHz) nuclear magnetic resonance (NMR) spectroscopic measurements were performed at 25 °C using a Bruker AV-400 spectrometer (Bruker, Silberstrifen, Germany) with tetramethylsilane as an internal standard in chloroform-*d* (CDCl$_3$).

The relative number- and weight-average molecular weights (M_n and M_w, respectively), as well as the molar-mass dispersity (M_w/M_n) of the polymers were estimated by gel permeation chromatographic (GPC) analysis. GPC measurements were obtained at 40 °C on a PC system equipped with a TSK gel SuperH-L guard column (Tosoh Bioscience, Tokyo, Japan), three columns (α-6000, α-4000 and α-2500) and a 2414 refractive index detector (Waters, Milford, MA, USA), tungsten lamp, wavelength 470–950 nm). Tetrahydrofuran was used as the eluent at a flow rate of 1.0 ml min^{-1}. Seven polystyrene standards ($M_n = 1060$–$3\,690\,000$, $M_w/M_n = 1.02$–1.08) were used to calibrate the GPC system.

X-ray photoelectron spectroscopy (XPS) measurements were performed using an XPS-APEX (Physical Electronics, Chanhassen, MN, USA) $<10^{-8}$ Torr, with a monochromatic Al-K$_\alpha$ X-ray source operating at 150 or 200 W.

The X-ray beam was focused on an area with a diameter of *ca.* 1.2 mm. The take-off angle of the photoelectrons was maintained at 45°, and a low-energy (25 eV) electron flood gun was used to minimize sample charging. The survey spectra were obtained over the range of 0–1000 at 1.0 eV energy steps. The narrow scans were performed with 0.1 eV energy steps.

Thermogravimetric analysis was conducted using a DTG-60 (Shimadzu Corporation, Kyoto, Japan). The heating rate was set at $10\,^{\circ}C\,min^{-1}$.

Preparation of dynamic covalent polymer brushes with alkoxyamine side chains on SiNPs (PMMA-*co*-PALMA-SiNP, 2)

A radically reactive polymer brush with alkoxyamine side chains was prepared using surface-initiated atom transfer radical polymerization (SI-ATRP, Scheme 1). The surface initiator, BHE, was synthesized by hydrosilylation of 5-hexenyl 2-bromoisobutylate treated with triethoxysilane, as previously reported.[12,21] BHE was immobilized on SiNPs (100 nm in diameter) using an ammonia-assisted method.[21] Finally, the nanoparticles modified with surface initiator (BHE-SiNP) were dispersed in trifluoroethanol to obtain a 10 wt% suspension.[22] Copolymerization of MMA and the alkoxyamine monomer ALMA(1) (copolymerization feed ratio, MMA/ALMA(1) = 10/1) was performed to obtain the corresponding dynamic covalent polymer brush by SI-ATRP. The suspension of BHE-SiNP (2 g with 200 mg of BHE-SiNP) was charged into a glass tube, and then, the trifluoroethanol solution of MMA (2.5 g, 25 mmol) and ALMA(1) (1.08 g, 2.5 mmol) was added slowly to prevent aggregation of SiNP. The mixture was ultrasonicated for 1 min, degassed by seven freeze–pump–thaw cycles, and backfilled with Ar gas. To the mixture, a degassed trifluoroethanol solution of CuBr (19.7 mg, 0.138 mmol) and 4,4′-dinonyl-N,N′-bipyridyl (112.3 mg, 0.275 mmol) was added under Ar flow. The mixture was again degassed by seven freeze–pump–thaw cycles. The free initiator, ethyl 2-bromoisobutyrate (20.1 μl, 0.135 mmol), was added to the mixture, and the glass tube was immersed in a thermostated oil bath maintained at 50 °C under Ar. After 15 h, the mixture was quenched to the liquid N_2 temperature and exposed to air. The mixture was then repeatedly centrifuged and dispersed with good solvents to remove the non-grafted free polymers and other low-molecular-weight molecules. Polymer brush-grafted SiNPs (PMMA-*co*-PALMA-SiNP, 2) were collected and dried under vacuum at 40 °C; 2 was obtained as a white solid. In addition, the supernatant was passed through an alumina column to remove the Cu catalyst and was then poured into excess methanol to collect the free (non-grafted) polymer that had been initiated by ethyl 2-bromoisobutyrate. The precipitate was then collected and dried *in vacuo*. The purified polymer was obtained as a white powder. In addition, a poly(methyl methacrylate) (PMMA) polymer brush on SiNP (PMMA-SiNP) without dynamic covalent bonds was also prepared as a control sample and was purified using the same procedure. For further examination, the grafted dynamic covalent polymer chains were cleaved from SiNP by HF etching and were characterized by NMR and GPC measurements.

Grafting reaction of fluoropolymer to PMMA-*co*-PALMA-SiNP (2)

PMMA-*co*-PALMA-SiNP (2, 20 mg) was charged into a glass tube and was maintained under reduced pressure to remove the air. Then, Ar was purged into the glass tube, and 0.5 ml of an anisole solution of alkoxyamine-terminated poly(2,3,4,5,6-pentafluorostyrene) (PPFS (3), 5 mg, 2.7 μmol ml^{-1}, $M_{n,GPC}=3700$) prepared by NMRP[14] was charged into the tube. The mixture was ultrasonicated for 1 min, degassed by seven freeze–pump–thaw cycles and sealed off under vacuum. The system was heated at 100 °C for 24 h. After the reaction, the particles were purified by repeating the centrifugation and re-dispersion processes with chloroform, and finally, the particles were dried *in vacuo*. The corresponding polymer-grafted SiNP (PMMA-*co*-PALMA-*g*-PPFS-SiNP, 4) was analyzed by XPS and dispersibility testing.

In addition, as a reference, the above experiment was performed using PMMA-SiNP instead of PMMA-*co*-PALMA-SiNP (2).

De-grafting reaction of PPFS from PMMA-*co*-PALMA-*g*-PPFS-SiNP (4)

PMMA-*co*-PALMA-*g*-PPFS-SiNP (4, 10 mg) was charged into a glass tube and was maintained under reduced pressure. After the glass tube was purged with Ar, an anisole solution (0.25 ml) of alkoxyamine 5 (9.8 mg, 0.13 mmol ml^{-1},

50 equiv. to PPFS) was added. The mixture was degassed by seven freeze–pump–thaw cycles and sealed off under vacuum. The solution was heated at 100 °C for 24 h. The physically adsorbed polymer was removed from the surface by repeated centrifugation and re-dispersion. The nanoparticles with PMMA-*co*-PALMA-SiNP (6) were then dried *in vacuo* and were analyzed by XPS.

Grafting reaction of poly(4-vinylpyridine) to PMMA-*co*-PALMA-SiNP (2)

A glass tube was charged with PMMA-*co*-PALMA-SiNP (2, 20 mg) and was maintained under reduced pressure to remove air. After the glass tube was purged with Ar, it was charged with a dimethylformamide solution (0.5 ml) of alkoxyamine-terminated poly(4-vinylpyridine) (P4VP(7), 5 mg, 1.4 μmol ml^{-1}, $M_{n,NMR}=6900$) prepared by NMRP.[14] The mixture was ultrasonicated for 1 min and degassed by seven freeze–pump–thaw cycles and sealed off under vacuum. The system was heated at 100 °C for 24 h. After the reaction, the particles were purified by repeating the centrifugation and re-dispersion processes with chloroform. Finally, the particles were dried *in vacuo*. The corresponding PMMA-*co*-PALMA-*g*-P4VP-SiNP (8) was analyzed by XPS.

In addition, as a reference, the above experiment was performed using PMMA-SiNP instead of PMMA-PALMA-SiNP.

Quaternization of pyridine moieties

PMMA-*co*-PALMA-*g*-P4VP-SiNP (8) was charged into a sample tube followed by iodomethane in tetrahydrofuran (1 ml, 0.1 M). The solution was maintained at room temperature in the dark for 24 h, and the solution was then removed. The obtained particles were dried under reduced pressure to remove any unreacted iodomethane and remaining solvent. The quaternized poly(4-vinylpyridine) (QP4VP)-grafted SiNP (PMMA-*co*-PALMA-*g*-QP4VP-SiNP, 9) was analyzed by XPS and dispersibility testing.

De-grafting reaction of QP4VP from PMMA-*co*-PALMA-*g*-QP4VP-SiNP (9)

A glass tube was charged with PMMA-*co*-PALMA-*g*-QP4VP-SiNP (9, 8 mg) and was maintained under reduced pressure. The tube was purged with Ar, and then alkoxyamine 5 in dimethylformamide (0.4 ml, 16.9 mg, 0.144 mmol ml^{-1}, 100 equiv. to QP4VP) was added. The mixture was degassed by seven freeze–pump–thaw cycles and sealed off under vacuum. The solution was heated at 100 °C for 24 h. The physically adsorbed polymer was removed from the surface by repeated centrifugation and re-dispersion processes. Then, PMMA-*co*-PALMA-SiNP (10) was dried *in vacuo* and analyzed by XPS.
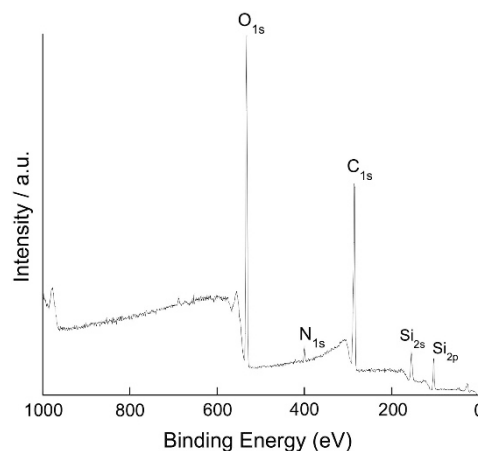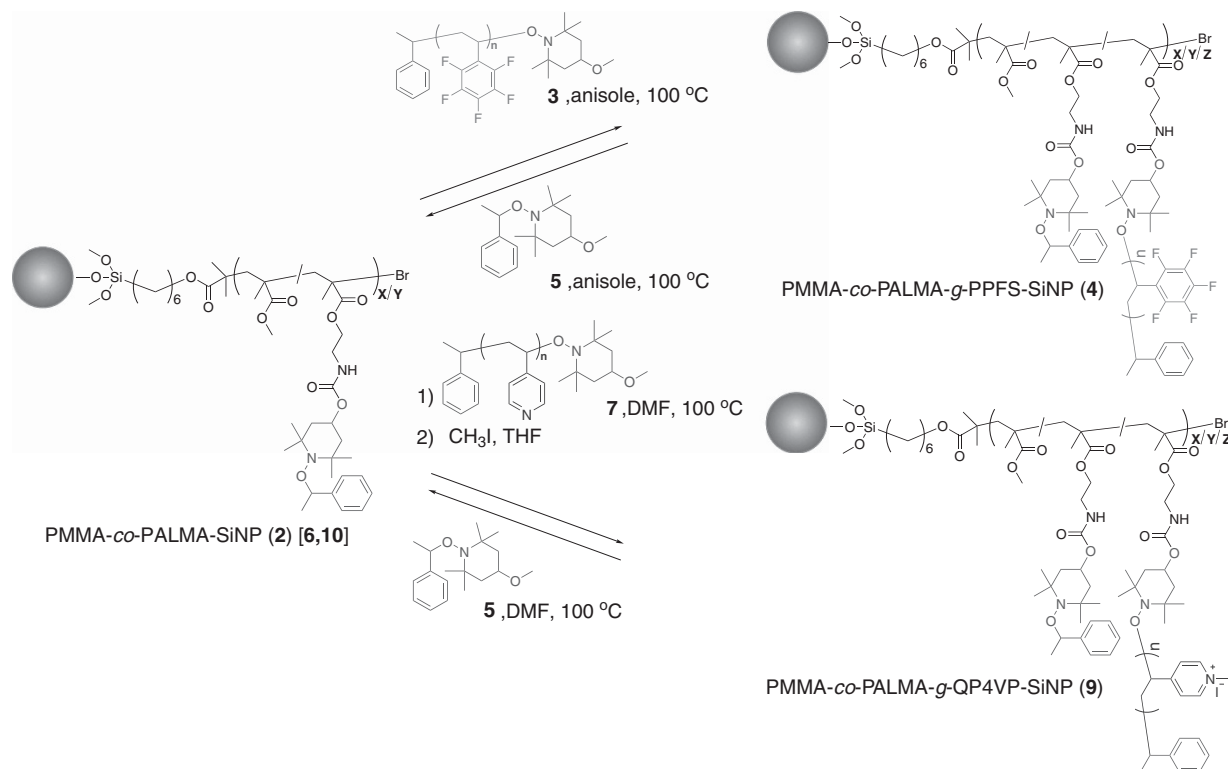

Figure 2 Wide-scan XPS spectrum of PMMA-*co*-PALMA-SiNP (2). PMMA, poly(methyl methacrylate); SiNP, silica nanoparticle; XPS, X-ray photoelectron spectroscopy.

RESULTS AND DISCUSSION

Preparation and characterization of the dynamic covalent polymer brushes on SiNP

PMMA-*co*-PALMA-SiNP (**2**) was prepared by SI-ATRP, as shown in Scheme 1. The M_n and M_w/M_n values for the PMMA-*co*-PALMA initiated by the free initiator were 5700 and 1.34, respectively. Furthermore, the M_n and M_w/M_n values of the polymers cleaved from the silica surface by HF etching showed similar values ($M_n = 7700$ and $M_w/M_n = 1.39$). In addition, no macroscopic side reactions, such as gelation or the appearance of a red color of nitroxides from free polymer, were observed. The structures of the obtained polymers were fully characterized by ^{1}H NMR. The compositions of the free polymer and of the cleaved polymer (PMMA-*co*-PALMA) were estimated as MMA/ALMA = 9.3/1 and 9.4/1, respectively. These results indicate that the copolymerization of ALMA(**1**) and MMA from the nanoparticles using SI-ATRP was successful. The estimated graft density, calculated from a previous method,[22] was 0.19 chains per nm², indicating that the polymer brush can be classified as the high-density type. In addition, the surface chemical composition for the dynamic covalent polymer brush on

Scheme 2 Scheme 2Radical crossover reaction of alkoxyamine moieties on a silica surface. DMF, dimethylformamide; PMMA, poly(methyl methacrylate); PPFS, poly(2,3,4,5,6-pentafluorostyrene); SiNP, silica nanoparticle; THF, tetrahydrofuran. A full color version of this scheme is available at *Polymer Journal* online.
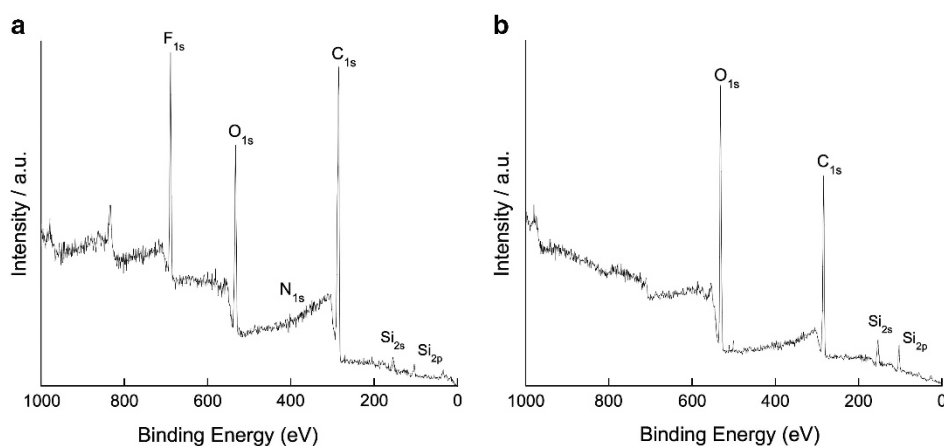

Figure 3 Wide-scan XPS spectra of (**a**) PMMA-*co*-PALMA-*g*-PPFS-SiNP (**4**) and (**b**) PMMA-SiNP after heating with PPFS (**3**) purified in a similar manner. PMMA, poly(methyl methacrylate); PPFS, poly(2,3,4,5,6-pentafluorostyrene); SiNP, silica nanoparticle; XPS, X-ray photoelectron spectroscopy.

SiNP was investigated by XPS. Figure 2 shows the wide-scan XPS spectrum of PMMA-*co*-PALMA-SiNP (**2**), which confirms the presence of nitrogen atoms of the alkoxyamine units and urethane bonds on the surface. The copolymerization ratio estimated from nitrogen and carbon peaks was MMA/ALMA = 8.8/1, which is slightly lower but is still a similar value compared with the monomer feed ratio.

Grafting reaction of fluoropolymer to nanoparticles by the dynamic covalent exchange of alkoxyamines

The grafting reaction of a fluorinated polymer to PMMA-*co*-PALMA-SiNP (**2**) was demonstrated via a dynamic covalent exchange reaction between alkoxyamines, as shown in Scheme 2. Through this reaction, the side chains of the polymer brush can be converted to fluorinated polymer chains, and a grafted copolymer brush can be obtained. Figure 3a shows the wide-scan XPS spectrum of PMMA-*co*-PALMA-*g*-PPFS-SiNP (**4**). After grafting, peaks assignable to fluorine atoms appeared in the spectrum of PMMA-*co*-PALMA-*g*-PPFS-SiNP (**4**) because the fluorinated chains exist on the surface of nanoparticles. To confirm that the appearance of fluorine atoms resulted from the dynamic covalent exchange, a reference XPS measurement of PMMA-
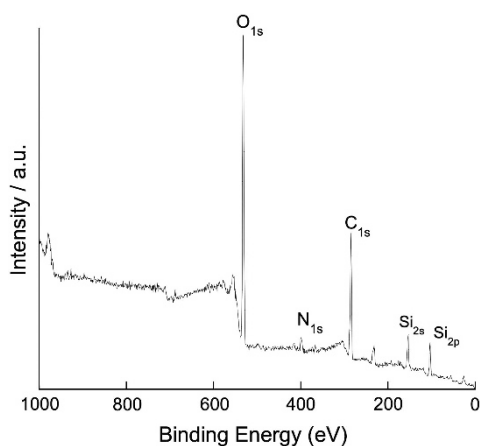
SiNP after the same treatment was performed. As shown in Figure 3b, there are no fluorine peaks in the spectrum of the reference nanoparticles. From these results, the peak appearance of fluorine is due to the dynamic covalent exchange of alkoxyamines between the side chains of PMMA-*co*-PALMA-SiNP (**2**) and the chain end of PPFS (**3**). The degree of exchange calculated from the peak ratio of the XPS spectrum was 9.7%. This relatively small value was caused by the steric hindrance of the polymer brush chains. The effective graft density (σ_{eff}), which is the graft density of chain ends, was calculated as 0.16 chains per nm^2, using a previously reported method.[73] This relatively high graft density also indicates that the size exclusion effect had a significant influence on the grafting reactions. These results confirmed that the grafting reaction of PPFS (**3**) to the nanoparticles occurred via a dynamic covalent exchange process, and the fluorinated chains would be introduced on the outer surface of the brush.[69]

De-grafting reaction of PPFS from nanoparticles by dynamic covalent exchange

The de-grafting reaction of PPFS chains from PMMA-*co*-PALMA-*g*-PPFS-SiNP (**4**) was performed to confirm the reversibility of the present dynamic covalent system. PMMA-*co*-PALMA-*g*-PPFS-SiNP (**4**) was treated with an excess amount of small molecular alkoxyamine **5** in solution at 100 °C for 24 h. Figure 4 shows the wide-scan XPS spectrum of the de-grafted SiNP, **6**, after the radical crossover reaction with alkoxyamine **5**. The XPS spectrum shows the peaks indicative of the elements C, N and O; however, the peaks from fluorine completely disappeared from the spectrum after the de-grafting reaction. Furthermore, the elemental ratios of **6** were nearly the same as the initial PMMA-PALMA-SiNP (**2**). These results indicate that the fluorinated side chains were removed by radical exchange de-grafting, thus converting the SiNP surface structure back to that of the original brush.

Grafting reaction of poly(4-vinylpyridine) to nanoparticles by the dynamic covalent exchange of alkoxyamines

We also grafted alkoxyamine-terminated P4VP to PMMA-*co*-PALMA-SiNP (**2**) to demonstrate the flexibility of this system (Scheme 2). Figure 5a shows the wide-scan XPS spectrum of PMMA-*co*-PALMA-*g*-P4VP-SiNP (**8**). The surface chemical composition of carbon and nitrogen was altered after grafting. The ratio of nitrogen to carbon (N/C = 0.069) showed a 1.8-fold increase compared with that before grafting. In contrast, the reference PMMA-SiNP showed no increase,
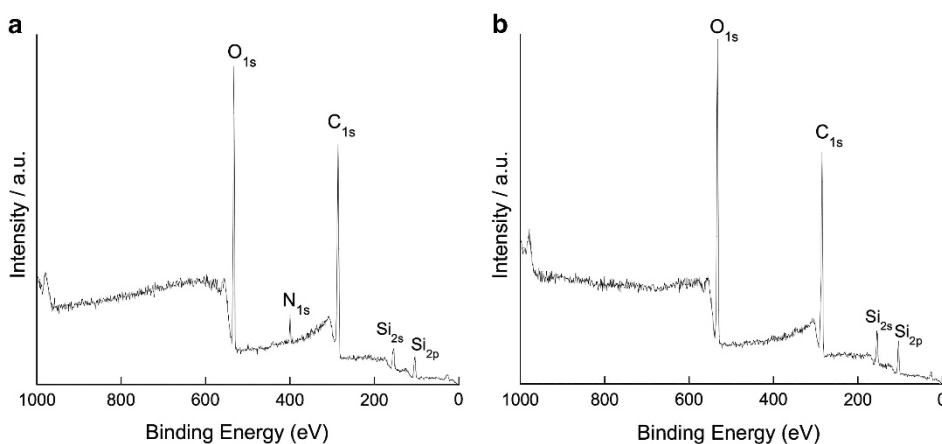
Figure 4 Wide-scan XPS spectrum of PMMA-*co*-PALMA-SiNP (**6**) after de-grafting of PPFS from PMMA-*co*-PALMA-*g*-PPFS-SiNP (**4**). PMMA, poly (methyl methacrylate); PPFS, poly(2,3,4,5,6-pentafluorostyrene); SiNP, silica nanoparticle; XPS, X-ray photoelectron spectroscopy.

Figure 5 Wide-scan XPS spectra of (**a**) PMMA-*co*-PALMA-*g*-P4VP-SiNP (**8**) and (**b**) PMMA after heating with P4VP and purified in a similar manner. PMMA, poly(methyl methacrylate); SiNP, silica nanoparticle; XPS, X-ray photoelectron spectroscopy.

as shown in Figure 5b. This indicates that carbon–nitrogen compounds were attached to PMMA-co-PALMA-SiNP (2). The grafting value was 2.2% due to the sterically hindered polymer brush chains. In addition, compared with fluorinated polymer grafting, this value was relatively small because of the difference in the molecular size between PPFS and P4VP used in this study.
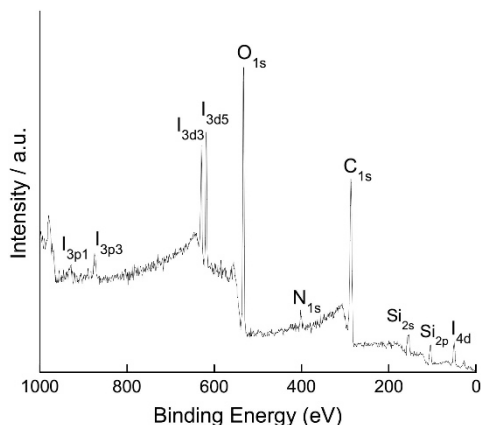

Figure 6 Wide-scan XPS spectrum of PMMA-co-PALMA-g-QP4VP-SiNP (9) after the quaternization reaction. PMMA, poly(methyl methacrylate); SiNP, silica nanoparticle; XPS, X-ray photoelectron spectroscopy.

Quaternization of P4VP side chains

To promote the hydrophilicity, quaternization of the P4VP chains was performed. Figure 6 shows the wide-scan XPS spectrum of PMMA-co-PALMA-g-QP4VP-SiNP (9) after the treatment of PMMA-co-PALMA-g-P4VP-SiNP (8) with iodomethane. The XPS spectra show the presence of iodine. Figures 7a–c show the narrow-scan XPS N_{1s} peak for nanoparticles 2, 8 and 9, respectively. Quaternization led to a broadening of the N_{1s} peak, as shown in Figure 7c, because of the appearance of the higher energy quaternary nitrogen peak and the diminishing neutral nitrogen peak. The changes in peak shape and position indicated that a high degree of quaternization occurred. In addition, the ratio of nitrogen to carbon ($N/C = 0.064$) was smaller because of the increment of carbon atoms by quaternization with iodomethane. The grafting ratio of the hydrophilic side chains was estimated as 2.3% from the surface chemical composition, which is nearly equal to the grafting value estimated from the chemical composition before the quaternization reaction.

De-grafting reaction of QP4VP from nanoparticles by dynamic covalent exchange

De-grafting of QP4VP (QP4VP) chains was also investigated. PMMA-co-PALMA-g-QP4VP-SiNP (9) was treated with an excess amount of the small molecular alkoxyamine 5 at 100 °C for 24 h. The XPS
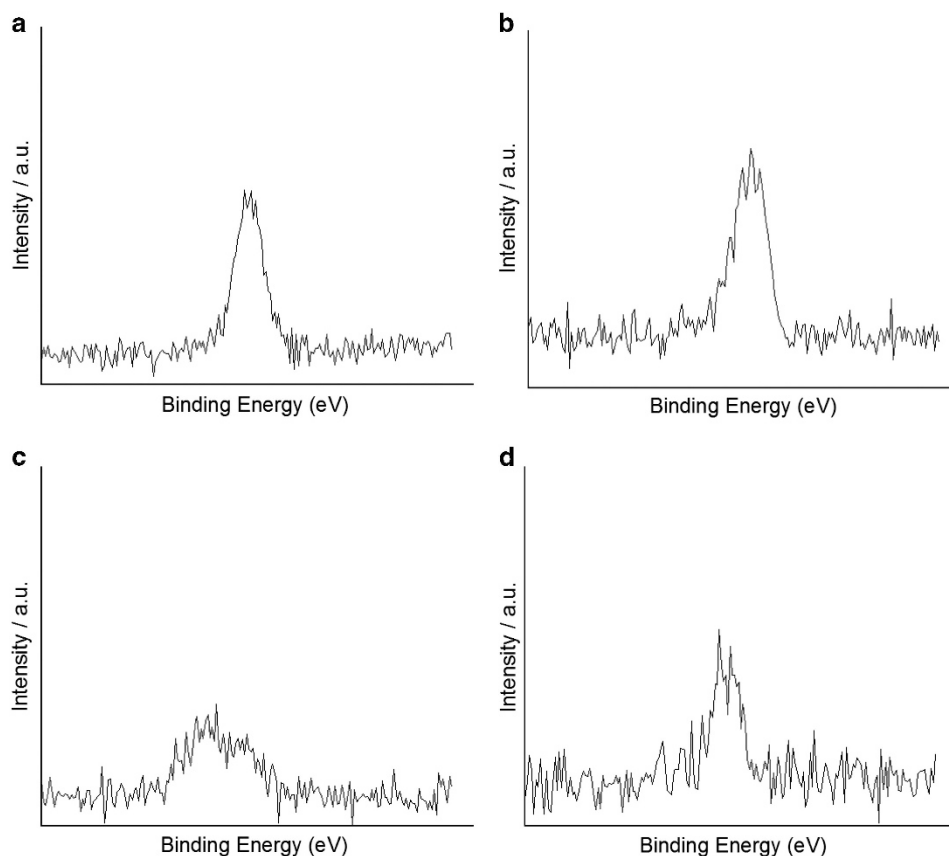

Figure 7 Narrow-scan XPS spectra of nitrogen (from 390 to 410 eV for (a) PMMA-co-PALMA-SiNP (2), (b) PMMA-co-PALMA-g-P4VP-SiNP (8), (c) PMMA-co-PALMA-g-QP4VP-SiNP (9) and (d) PMMA-co-PALMA-SiNP (10). PMMA, poly(methyl methacrylate); SiNP, silica nanoparticle; XPS, X-ray photoelectron spectroscopy.

spectrum of the SiNP after de-grafting is shown in Figure 8. Peaks are present for C, N and O but not for iodine, indicating that it has been completely removed from the surface. Furthermore, the peak for N_{1s} on XPS spectrum became narrow, and the shape of the spectrum changed to that of the original PMMA-*co*-PALMA-SiNP (**2**), as shown in Figure 7d. The elemental ratio of the de-grafted SiNP **10** is similar to the original SiNP **2** (N/C = 0.042) and was 0.6 times lower than that of PMMA-*co*-PALMA-*g*-P4VP-SiNP (**8**).

Dispersibility of nanoparticles

The grafted polymer chains determine the nanoparticle dispersibility. Figure 9 shows the photographs for the dispersion of PPFS- and QP4VP-modified SiNP (**4** and **9**, respectively) in water. Due to the difference in affinity of the polymer chains for water, the two polymer-grafted SiNPs showed distinct dispersion behaviors. QP4VP-grafted SiNP **9** was well dispersed because of the size exclusion effects of the hydrated hydrophilic polymer chains. However, the PPFS-grafted SiNP **4** aggregates because the hydrophobic chains shrink in water. This indicates that the dispersibility of the SiNPs was dramatically altered by the grafting reactions. Further insight into the particle dispersion was investigated by the dispersibility tests of the SiNPs for various solvents. Table 1 summarizes the dispersibility of polymer-grafted nanoparticles in four solvents: water, chloroform, methanol
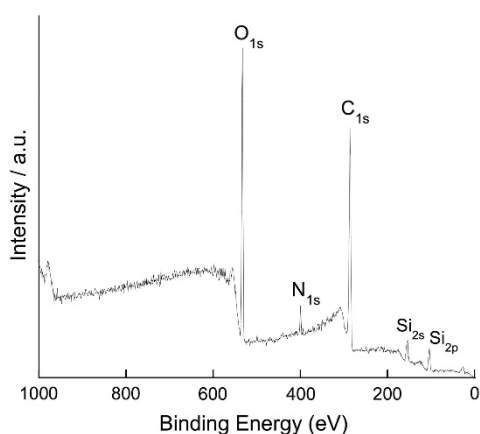
and *n*-hexane. These experiments confirmed that the dispersibility of the nanoparticles depends on the properties of the grafted chains. Good solvents for the polymer brushes lead to good dispersibility. For example, PPFS-grafted SiNP **4** can disperse in chloroform and ethyl acetate, which are good solvents for the PPFS chains. In contrast, PPFS-grafted SiNP **4** aggregates in water and hexane. In all cases, the de-grafting achieves a similar dispersibility to the initial particles.

CONCLUSION

We demonstrated the reversible grafting of functional polymers to nanoparticles via the dynamic covalent exchange reaction of alkoxyamine-appended polymer brushes. The dynamic covalent polymer brushes with radically exchangeable side chains were prepared on SiNPs using SI-ATRP. Radical crossover reactions were used to reversibly exchange the side chains with fluorinated polymers or ionic polymers. The chemical composition of the altered polymer brushes was characterized by XPS measurements. In addition, the polymer-grafted nanoparticles showed different dispersibility in solutions, depending on the grafted polymer chains. Furthermore, the introduced polymer chains were removed by the radical exchange reactions with an excess amount of small molecular alkoxyamine. These findings indicate that the nanoparticle dispersion was controlled by a combination of using dynamic covalent polymer brushes and the subsequent 'grafting to' procedure. The reactions demonstrated in this study can be used for the reversible and desirable surface modification of nanomaterials, and they are appropriate for various applications that require changes in dispersibility by functional group alteration.

Figure 8 Wide-scan XPS spectrum of PMMA-*co*-PALMA-SiNP (**10**) after de-grafting of QP4VP from PMMA-*co*-PALMA-*g*-QP4VP-SiNP (**9**). PMMA, poly(methyl methacrylate); SiNP, silica nanoparticle; XPS, X-ray photoelectron spectroscopy.

Table 1 Relative dispersibility of polymer-grafted nanoparticles[a]

	Water	Methanol	Chloroform	n-Hexane
PMMA-PALMA-grafted SiNP **2**	−	−	+	−
PPFS-grafted SiNP **4**	−	−	+	−
QP4VP-grafted SiNP **9**	++	+	+	−

Abbreviations: PMMA, poly(methyl methacrylate); PPFS, poly(2,3,4,5,6-pentafluorostyrene); QP4VP, quaternized poly(4-vinylpyridine); SiNP, silica nanoparticle.
[a]The dispersion behavior of polymer-grafted SiNP for the different solvents was investigated as follows: glass tubes were charged with each SiNP sample (2 mg) and each solvent (1 ml). The mixture was then ultrasonicated for 1 min. The dispersibility was evaluated by visual comparison and by laser scattering.
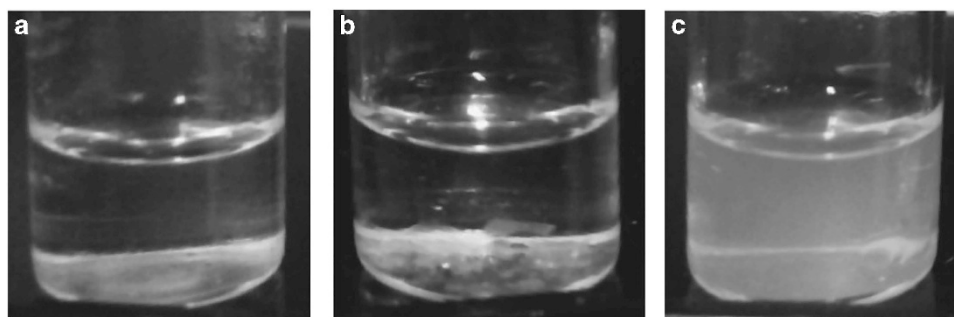Key: ++, well dispersed; +, partially aggregated; −, almost aggregated.

Figure 9 Photographs of water suspension of polymer brush-modified nanoparticles: (**a**) PMMA-*co*-PALMA-SiNP (**2**), (**b**) PMMA-*co*-PALMA-*g*-PPFS-SiNP (**4**) and (**c**) PMMA-*co*-PALMA-*g*-QP4VP-SiNP (**9**). PMMA, poly(methyl methacrylate); PPFS, poly(2,3,4,5,6-pentafluorostyrene); QP4VP, quaternized poly(4-vinylpyridine); SiNP, silica nanoparticle. A full color version of this figure is available at *Polymer Journal* online.

CONFLICT OF INTEREST

The authors declare no conflict of interest.

ACKNOWLEDGEMENTS

1 Gupta, A. K. & Gupta, M. Synthesis and surface engineering of iron oxide nanoparticles for biomedical applications. *Biomaterials* **26**, 3995–4021 (2005).

2 Kawasumi, M., Hasegawa, N., Kato, M., Usuki, A. & Okada, A. Preparation and mechanical properties of polypropylene-clay hybrids. *Macromolecules* **30**, 6333–6338 (1997).

3 Paul, D. R. & Robeson, L. M. Polymer nanotechnology: nanocomposites. *Polymer* **49**, 3187–3204 (2008).

4 Sinha Ray, S. & Okamoto, M. Polymer/layered silicate nanocomposites: a review from preparation to processing. *Prog. Polym. Sci.* **28**, 1539–1641 (2003).

5 Milner, S. T. Polymer brushes. *Science* **251**, 905–914 (1991).

6 Zhao, B. & Brittain, W. J. Polymer brushes: surface-immobilized macromolecules. *Prog. Polym. Sci.* **25**, 677–710 (2000).

7 Edmondson, S., Osborne, V. L. & Huck, W. T. S. Polymer brushes via surface-initiated polymerizations. *Chem. Soc. Rev.* **33**, 14–22 (2004).

8 Ejaz, M., Yamamoto, S., Ohno, K., Tsujii, Y. & Fukuda, T. Controlled graft polymerization of methyl methacrylate on silicon substrate by the combined use of the langmuir-blodgett and atom transfer radical polymerization techniques. *Macromolecules* **31**, 5934–5936 (1998).

9 Husseman, M. M., Eva, E., McNamara, M., Mate, M., Mecerreyes, D., Benoit, D. G., Hedrick, J. L., Mansky, P., Huang, E., Russell, T. P. & Hawker, C. J. Controlled synthesis of polymer brushes by 'living' free radical polymerization techniques. *Macromolecules* **32**, 1424–1431 (1999).

10 Kato, K., Uchida, E., Kang, E. -T., Uyama, Y. & Ikada, Y. Polymer surface with graft chains. *Prog. Polym. Sci.* **28**, 209–259 (2003).

11 Zhao, B. & Brittain, W. J. Synthesis of tethered polystyrene-block-poly(methyl methacrylate) monolayer on a silicate substrate by sequential carbocationic polymerization and atom transfer radical polymerization. *J. Am. Chem. Soc.* **121**, 3557–3558 (1999).

12 Sakata, H., Kobayashi, M., Otsuka, H. & Takahara, A. Tribological properties of poly (methyl methacrylate) brushes prepared by surface-initiated atom transfer radical polymerization. *Polym. J.* **37**, 767–775 (2005).

13 Bielawski, C. W. & Grubbs, R. H. Living ring-opening metathesis polymerization. *Prog. Polym. Sci.* **32**, 1–29 (2007).

14 Hawker, C. J., Bosman, A. W. & Harth, E. New polymer synthesis by nitroxide mediated living radical polymerizations. *Chem. Rev.* **101**, 3661–3688 (2001).

15 Kamigaito, M., Ando, T. & Sawamoto, M. Metal-catalyzed living radical polymerization. *Chem. Rev.* **101**, 3689–3745 (2001).

16 Matyjaszewski, K. & Xia, J. Atom transfer radical polymerization. *Chem. Rev.* **101**, 2921–2990 (2001).

17 Li, L., Davidson, J. L. & Lukehart, C. M. Surface functionalization of nanodiamond particles via atom transfer radical polymerization. *Carbon* **44**, 2308–2315 (2006).

18 Matsuno, R., Otsuka, H. & Takahara, A. Polystyrene-grafted titanium oxide nanoparticles prepared through surface-initiated nitroxide-mediated radical polymerization and their application to polymer hybrid thin films. *Soft. Matter* **2**, 415–421 (2006).

19 Matsuno, R., Yamamoto, K., Otsuka, H. & Takahara, A. Polystyrene-grafted magnetite nanoparticles prepared through surface-initiated nitroxyl-mediated radical polymerization. *Chem. Mater.* **15**, 3–5 (2003).

20 Ohno, K., Koh, K., Tsujii, Y. & Fukuda, T. Fabrication of ordered arrays of gold nanoparticles coated with high-density polymer brushes. *Angew. Chem. Int. Ed.* **42**, 2751–2754 (2003).

21 Ohno, K., Morinaga, T., Koh, K., Tsujii, Y. & Fukuda, T. Synthesis of monodisperse silica particles coated with well-defined, high-density polymer brushes by surface-initiated atom transfer radical polymerization. *Macromolecules* **38**, 2137–2142 (2005).

22 Kikuchi, M., Terayama, Y., Ishikawa, T., Hoshino, T., Kobayashi, M., Ogawa, H., Masunaga, H., Koike, J., Horigome, M., Ishihara, K. & Takahara, A. Chain dimension of polyampholytes in solution and immobilized brush states. *Polym. J.* **44**, 121–130 (2012).

23 Chen, T., Ferris, R., Zhang, J., Ducker, R. & Zauscher, S. Stimulus-responsive polymer brushes on surfaces: transduction mechanisms and applications. *Prog. Polym. Sci.* **35**, 94–112 (2010).

24 Horton, J. M., Bao, C., Bai, Z., Lodge, T. P. & Zhao, B. Temperature- and pH-triggered reversible transfer of doubly responsive hairy particles between water and a hydrophobic ionic liquid. *Langmuir.* **27**, 13324–13334 (2011).

25 Huang, S., Guo, X., Li, L. & Dong, Y. Volume transition and adhesion force of nanosized bifunctional spherical polyelectrolyte brushes observed by dynamic light scattering and atomic force microscopy. *J. Phys. Chem. B* **116**, 10079–10088 (2012).

26 Li, D., He, Q., Yang, Y., Möhwald, H. & Li, J. Two-stage pH response of poly(4-vinylpyridine) grafted gold nanoparticles. *Macromolecules* **41**, 7254–7256 (2008).

27 Li, D., Sheng, X. & Zhao, B. Environmentally responsive 'hairy' nanoparticles: mixed homopolymer brushes on silica nanoparticles synthesized by living radical polymerization techniques. *J. Am. Chem. Soc.* **127**, 6248–6256 (2005).

28 Mazurowski, M., Gallei, M., Li, J., Didzoleit, H., Stühn, B. & Rehahn, M. Redox-responsive polymer brushes grafted from polystyrene nanoparticles by means of surface initiated atom transfer radical polymerization. *Macromolecules* **45**, 8970–8981 (2012).

29 Matsui, J., Parvin, S., Sato, E. & Miyashita, T. Preparation of organic-ceramic-metal multihybrid particles and their organized assembly. *Polym. J.* **42**, 142–147 (2009).

30 Ito, M., Enomoto, R., Osawa, K., Daiko, Y., Yazawa, T., Fujii, S., Yokoyama, Y., Miyanari, Y., Nakamura, Y., Nakao, A., Iwasaki, Y. & Yusa, S. pH-responsive flocculation and dispersion behavior of Janus particles in water. *Polym. J.* **44**, 181–188 (2011).

31 Kobayashi, K., Wei, J., Iida, R., Ijiro, K. & Niikura, K. Surface engineering of nanoparticles for therapeutic applications. *Polym. J.* **46**, 460–468 (2014).

32 Kanazawa, H., Sunamoto, T., Ayano, E., Matsushima, Y., Kikuchi, A. & Okano, T. Temperature-responsive chromatography using poly(N-isopropylamide) hydrogel-modified silica. *Anal. Sci.* **18**, 45–48 (2002).

33 Kanazawa, H., Yamamoto, K. & Matsushima, Y. Temperature-responsive chromatography using poly(N-isopropylacrylamide)-modified silica. *Anal. Chem.* **68**, 100–105 (1996).

34 Kizhakkedathu, J. N., Norris-Jones, R. & Brooks, D. E. Synthesis of well-defined environmentally responsive polymer brushes by aqueous ATRP. *Macromolecules* **37**, 734–743 (2004).

35 Tamura, A., Nishi, M., Kobayashi, J., Nagase, K., Yajima, H., Yamato, M. & Okano, T. Simultaneous enhancement of efficiency based on temperature-responsive cationic copolymer-grafted microcarriers. *Biomacromolecules* **13**, 1765–1773 (2012).

36 Lehn, J. -M. From supramolecular chemistry towards constitutional dynamic chemistry and adaptive chemistry. *Chem. Soc. Rev.* **36**, 151–160 (2007).

37 Rowan, S. J., Cantrill, S. J., Cousins, G. R. L., Sanders, J. K. M. & Stoddart, J. F. Dynamic covalent chemistry. *Angew. Chem. Int. Ed.* **41**, 898–952 (2002).

38 Jin, Y., Yu, C., Denman, R. J. & Zhang, W. Recent advances in dynamic covalent chemistry. *Chem. Soc. Rev.* **42**, 6634–6654 (2013).

39 Wojtecki, R. J., Meador, M. A. & Rowan, S. J. Using the dynamic bond to access macroscopically responsive structurally dynamic polymers. *Nat. Chem.* **10**, 14–27 (2011).

40 Lehn, J. -M. Dynamers: dynamic molecular and supramolecular polymers. *Prog. Polym. Sci.* **30**, 814–831 (2005).

41 Maeda, T., Otsuka, H. & Takahara, A. Dynamic covalent polymers: reorganizable polymers with dynamic covalent bonds. *Prog. Polym. Sci.* **34**, 581–604 (2009).

42 Hawker, C. J., Barclay, G. G. & Dao, J. Radical crossover in nitroxide mediated 'living' free radical polymerizations. *J. Am. Chem. Soc.* **118**, 11467–11471 (1996).

43 Tebben, L. & Studer, A. Nitroxides: applications in synthesis and in polymer chemistry. *Angew. Chem. Int. Ed.* **50**, 5034–5068 (2011).

44 Otsuka, H. Reorganization of polymer structures based on dynamic covalent chemistry: polymer reactions by dynamic covalent exchanges of alkoxyamine units. *Polym. J.* **45**, 879–891 (2013).

45 Audran, G., Brémond, P. & Marque, S. R. A. Labile alkoxyamines: past, present, and future. *Chem. Commun.* **50**, 7921–7928 (2014).

46 Otsuka, H., Aotani, K., Higaki, Y., Amamoto, Y. & Takahara, A. Thermal reorganization and molecular weight control of dynamic covalent polymers containing alkoxyamines in their main chains. *Macromolecules* **40**, 1429–1434 (2007).

47 Otsuka, H., Aotani, K., Higaki, Y. & Takahara, A. A dynamic (reversible) covalent polymer: radical crossover behaviour of TEMPO-containing poly(alkoxyamine ester)s. *Chem. Commun.* 2838–2839 (2002).

48 Otsuka, H., Aotani, K., Higaki, Y. & Takahara, A. Polymer scrambling: macromolecular radical crossover reaction between the main chains of alkoxyamine-based dynamic covalent polymers. *J. Am. Chem. Soc.* **125**, 4064–4065 (2003).

49 Yamaguchi, G., Higaki, Y., Otsuka, H. & Takahara, A. Reversible radical ring-crossover polymerization of an alkoxyamine-containing dynamic covalent macrocycle. *Macromolecules* **38**, 6316–6320 (2005).

50 Higaki, Y., Otsuka, H. & Takahara, A. Dynamic formation of graft polymers via radical crossover reaction of alkoxyamines. *Macromolecules* **37**, 1696–1701 (2004).

51 Wang, G. & Huang, J. Versatility of radical coupling in construction of topological polymers. *Polym. Chem.* **5**, 277–308 (2014).

52 Amamoto, Y., Kikuchi, M., Masunaga, H., Ogawa, H., Sasaki, S., Otsuka, H. & Takahara, A. Mesh-size control and functionalization of reorganizable chemical gels by monomer insertion into their cross-linking points. *Polym. Chem.* **2**, 957–962 (2011).

53 Amamoto, Y., Kikuchi, M., Masunaga, H., Sasaki, S., Otsuka, H. & Takahara, A. Reorganizable chemical polymer gels based on dynamic covalent exchange and controlled monomer insertion. *Macromolecules* **42**, 8733–8738 (2009).

54 Higaki, Y., Otsuka, H. & Takahara, A. A thermodynamic polymer cross-linking system based on radically exchangeable covalent bonds. *Macromolecules* **39**, 2121–2125 (2006).

55 Su, J., Amamoto, Y., Nishihara, M., Takahara, A. & Otsuka, H. Reversible cross-linking of hydrophilic dynamic covalent polymers with radically exchangeable alkoxyamines in aqueous media. *Polym. Chem.* **2**, 2021–2026 (2011).

56 Su, J., Amamoto, Y., Sato, T., Kume, M., Inada, T., Ohishi, T., Higaki, Y., Takahara, A. & Otsuka, H. Reversible cross-linking reactions of alkoxyamine-appended polymers

under bulk conditions for transition between flow and rubber-like states. *Polymer* **55**, 1474–1480 (2014).

57 Su, J., Imato, K., Sato, T., Ohishi, T., Takahara, A. & Otsuka, H. Plasticizer-promoted thermal crosslinking of a dynamic covalent polymer with complementarily reactive alkoxyamine units in the side chain under bulk conditions. *Bull. Chem. Soc. Jpn* **87**, 1023–1025 (2014).

58 Amamoto, Y., Higaki, Y., Matsuda, Y., Otsuka, H. & Takahara, A. Programmed thermodynamic formation and structure analysis of star-like nanogels with core cross-linked by thermally exchangeable dynamic covalent bonds. *J. Am. Chem. Soc.* **129**, 13298–13304 (2007).

59 Amamoto, Y., Maeda, T., Kikuchi, M., Otsuka, H. & Takahara, A. Rational approach to star-like nanogels with different arm lengths: formation by dynamic covalent exchange and their imaging. *Chem. Commun.* 689–691 (2009).

60 Becker, M., Cola, L. D. & Studer, A. Site-specific immobilization of proteins at zeolite L crystals by nitroxide exchange reactions. *Chem. Commun.* **47**, 3392–3394 (2011).

61 Blinco, J. P., Trouillet, V., Bruns, M., Gerstel, P., Gliemann, H. & Barner-Kowollik, C. Dynamic covalent chemistry on surfaces employing highly reactive cyclopentadienyl moieties. *Adv. Mater.* **23**, 4435–4439 (2011).

62 Jhaveri, S. B., Beinhoff, M., Hawker, C. J., Carter, K. R. & Sogah, D. Y. Chain-end functionalized nanopatterned polymer brushes grown via *in situ* nitroxide free radical exchange. *ACS Nano* **2**, 719–727 (2008).

63 Ono, T., Fujii, S., Nobori, T. & Lehn, J. -M. Optodynamers: expression of color and fluorescence at the interface between two films of different dynamic polymers. *Chem. Commun.* 4360–4362 (2007).

64 Rozkiewicz, D. I., Ravoo, B. J. & Reinhoudt, D. N. Reversible covalent patterning of self-assembled monolayers on gold and silicon oxide surfaces. *Langmuir.* **21**, 6337–6343 (2005).

65 Schulte, B., Tsotsalas, M., Becker, M., Studer, A. & De Cola, L. Dynamic microcrystal assembly by nitroxide exchange reactions. *Angew. Chem. Int. Ed.* **49**, 6881–6884 (2010).

66 Tauk, L., Schröder, A. P., Decher, G. & Giuseppone, N. Hierarchical functional gradients of pH-responsive self-assembled monolayers using dynamic covalent chemistry on surfaces. *Nat. Chem.* **1**, 649–656 (2009).

67 Wagner, H., Brinks, M. K., Hirtz, M., Schäfer, A., Chi, L. & Studer, A. Chemical surface modification of self-assembled monolayers by radical nitroxide exchange reactions. *Chem. Eur. J.* **17**, 9107–9112 (2011).

68 Sato, T., Amamoto, Y., Ohishi, T., Higaki, Y., Takahara, A. & Otsuka, H. Radical crossover reactions of a dynamic covalent polymer brush for reversible hydrophilicity control. *Polymer* **55**, 4586–4592 (2014).

69 Sato, T., Amamoto, Y., Yamaguchi, H., Ohishi, T., Takahara, A. & Otsuka, H. Dynamic covalent polymer brushes: reversible surface modification of reactive polymer brushes with alkoxyamine-based dynamic covalent bonds. *Polym. Chem.* **3**, 3077–3083 (2012).

70 Sato, T., Amamoto, Y., Yamaguchi, H., Otsuka, H. & Takahara, A. 'Substitutable' polymer brushes: reactive poly(methacrylate) brushes with exchangeable alkoxyamine units in the side chain. *Chem. Lett.* **39**, 1209–1211 (2010).

71 Jin, J., Liu, J., Lian, X., Sun, P. & Zhao, H. Dynamic polymer brushes on the surface of silica particles. *RSC Adv.* **3**, 7023–7029 (2013).

72 Leung, K. C. -F., Xuan, S. & Lo, C. -M. Reversible switching between hydrophilic and hydrophobic superparamagnetic iron oxide microspheres via one-step supramolecular dynamic dendronization: exploration of dynamic wettability. *ACS Appl. Mater. Interfaces* **1**, 2005–2012 (2009).

73 Ohno, K., Morinaga, T., Takeno, S., Tsujii, Y. & Fukuda, T. Suspensions of silica particles grafted with concentrated polymer brush: effects of graft chain length on brush layer thickness and colloidal crystallization. *Macromolecules* **36**, 9143–9150 (2007).